Investigation of Singularities in a 3/4 CMG Configuration with Mixed Skew Angles

Jonathan W. Lang

Abstract

This paper discusses the singularities that exist within a 3/4 CMG configuration when the CMGs are placed at mixed skew angles. CMGs are typically mounted with the same skew angles and are fixed throughout the spacecraft's lifetime. Changing these skew angles can bring about unique attributes for the spacecraft such as an increased pitch, roll or yaw capability. Mapping out these singularities when each CMG is mounted differently can show an engineer how to maximize these capabilities and enhance a spacecraft's mission completion ability. Using singularity penetration logic, the spacecraft's attitude controls system can pass through these singularities. These singularities would best be avoided to provide optimal control. Finding these limited singularity penetration regions is the focus of this paper. Different mixed skew configurations appear to be more ideal than others for spacecraft that focus on maneuvers about only one axis of rotation.

Keywords: mixed skew angles, 3/4 CMG configuration, singularity penetration, CMG configuration singularity regions

1. Introduction

CMGs have become a staple in the space community as a means to accomplish pointing, tracking, and acquiring. CMGs create a torque by rotating or "gimbaling" the CMGs angular momentum vector. The change in angular momentum is how the CMG produces torque and creates movement for the spacecraft.

The Torque axis (τ) rotation for a CMG is the axis around which the spacecraft maneuver is accomplished. The Torque Axis and the orthogonal relationship between the CMG's gimbal axis (δ) and angular momentum axis (H) can be seen in **Figure 1**. These relationships demonstrate how one may discover the Torque axis and provide the intuition behind singularity generation in this configuration [1].

2. CMG 3/4 configuration model

The 3/4 configuration will have the CMGs positioned in the same configuration around the spacecraft throughout the analysis in this paper and can be seen in **Figure 2**.

The 3/4 configuration [2] is a simple form of spacecraft CMG placement which provides an environment where singularities exist.
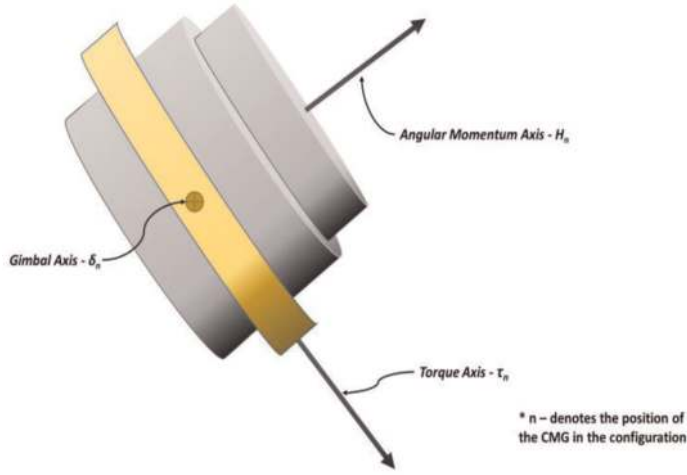
Figure 1.
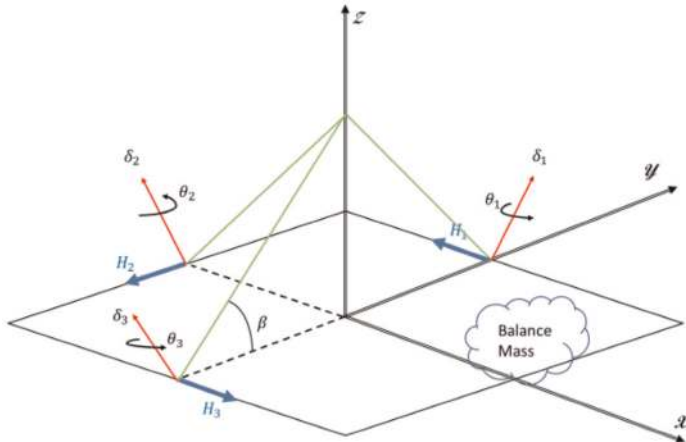*CMG angular momentum-torque-gimbal axis representation.*

Figure 2.
3/4 configuration of CMGs on a spacecraft.

All modeling in this project will be accomplished through MATLAB—Simulink modeling software. A step size of 0.001 s was found to be the most accurate while using ODE4 Runge-Kutta Integration Solver.

3. CMG angular momentum projected on the body reference axes

The three CMG's each have an angular momentum vector (H_i) which can be seen in **Figure 2** and is projected onto the x, y, z reference frame axes in Eqs. (1)–(3). These three vectors rotate about each of the CMG's gimbal axis (δ_i).

$$H_x = -H_1 \cos(\theta_1) + H_2 \cos(\beta_2) \sin(\theta_2) + H_3 \cos(\theta_3) \tag{1}$$

$$H_y = -H_1 \cos(\beta_1) \sin(\theta_1) - H_2 \cos(\theta_2) + H_3 \cos(\beta_3) \sin(\theta_3) \tag{2}$$

$$H_z = \sin(\beta_1)H_1 \sin(\theta_1) + \sin(\beta_2)H_2 \sin(\theta_2) + \sin(\beta_3)H_3 \sin(\theta_3) \tag{3}$$

A new matrix $[\mathbf{A}]$ made up of the spatial gradient of Eqs. (1)–(3) can be generated [2]. This new matrix is how singularities can be discovered numerically.

$$\frac{\partial H}{\partial \theta} = \left\{ \begin{array}{c} \partial H_x / \partial \theta_i \\ \partial H_y / \partial \theta_i \\ \partial H_z / \partial \theta_i \end{array} \right\} = [A]$$

$$[A] = \begin{bmatrix} sin\,(\theta_1) & cos\,(\beta_2)\,cos\,(\theta_2) & -sin\,(\theta_3) \\ -cos\,(\beta_1)\,cos\,(\theta_1) & sin\,(\theta_2) & cos\,(\beta_3)\,cos\,(\theta_3) \\ sin\,(\beta_1)\,cos\,(\theta_1) & sin\,(\beta_2)\,cos\,(\theta_2) & sin\,(\beta_3)\,cos\,(\theta_3) \end{bmatrix} \qquad (4)$$

Torque is generated by the time rate of change in the angular momentum, which may be expressed in a chain rule of derivatives and solved for the gimbal rates.

$$T = \dot{H}$$

$$\dot{H} = \frac{\partial H}{\partial \theta}\frac{d\theta}{dt}$$

$$\dot{H} = [A]\dot{\theta}$$

$$\dot{\theta} = [A]^{-1}\dot{H} \qquad (5)$$

Now there is a relationship between the time rate of change in the angular momentum ($\dot{H}$) and the time rate of change of gimbal axis rotation ($\dot{\theta}$) found in Eq. (5). The required gimbal axis rotation for a commanded torque may be applied for the appropriate spacecraft maneuver. The one possible danger associated with this is the inversion of the matrix $[A]$.

4. Accuracy of inverting the $[A]$ matrix

Inverting the $[A]$ matrix becomes an integral part of determining the creation of the gimbal axis rotation ($\dot{\theta}$) as seen in Eq. (5). Analysis was done on eight different inversion models, the principal one on which all others are compared was the Moore-Penrose matrix inversion [3]. The other seven cases are found in **Table 1**.

The $pinv([A])$ matrix inversion model turns out to be the best suited model as seen in **Table 1**. This seems to be intuitive since the $pinv\,([A])$ is a reiteration of the Moore-Penrose inversion.

Case	[A] Inversion model	Matrix-Norm difference
1	$[A]^{-1}$	0.872826646563208
2	$inv([A])$	0.872826646563208
3	$pinv([A])$	0
4	$[A]\,eye(size([A]))$	0.872826646560334
5	*LU Decomposition*	0.872826646560693
6	*Analytical Matrix*	6.67204727298e+04
7	*Analytical Formulas*	6.67204727298e+04

Table 1.
Matrix-norm difference between each case and the Moore-Penrose matrix inversion.

5. Applying CMG torque to the spacecraft

Now that the CMG torque has been developed it can now be applied to the spacecraft.

$$\tau = J\dot{\omega} + \omega \times J\omega \qquad (6)$$

Using Euler's dynamical Eq. (6), the angular momentum and cross-coupled disturbances can be used to determine the resulting three-axis rotation [4].

6. Singularity penetration logic

Singularity existence has been discussed at length in [2].

Singularities exist when the determinant of the [A] matrix from Eq. (4) approaches zero [2]. Penetration Logic takes advantage of the fact that as the inverse condition number approaches zero the singularity would be met. At a user defined threshold of 1 e-6 penetration logic tells the commanded Gimbal motor rates to repeat the last iteration (before the inverse condition number crossed the user defined threshold and reaches singularity), see **Figure 3**.
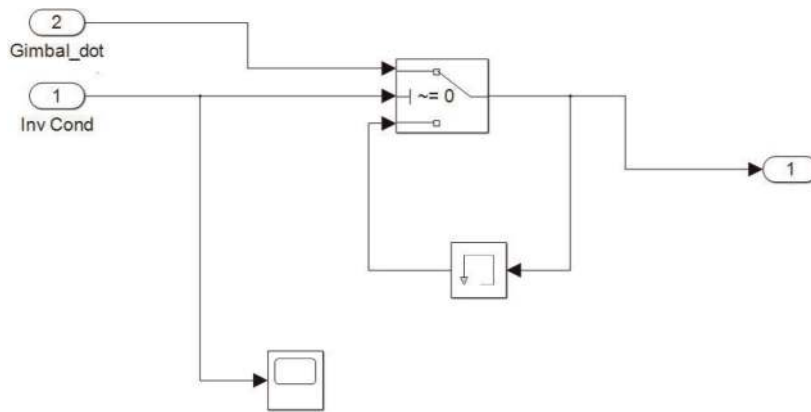
Figure 3.
Singularity penetration with unit delay logic.

7. PDI controller tuning

The PDI controller will be used to generate a control signal from the commanded input signal and the spacecraft feedback signal. The topography for the PDI controller can be seen in **Figure 4**.

The PDI controller accepts both the commanded angle and angular velocity as well as the feedback angle and angular velocity and avoids using the derivative function.

Tuning the gains become the next step in building the controller section of the spacecraft. Three different tuning techniques will be covered:
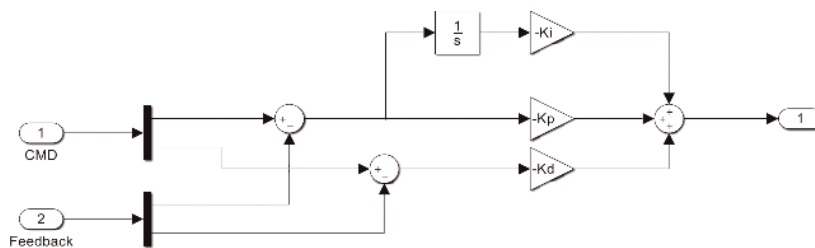
Figure 4.
PDI controller topography.

7.1 Ziegler-Nichols tuning

This tuning technique requires the gain margin (K_u) and bandwidth frequency (ω_b) for the system to be found. Once these two values are discovered the equations in (7) may be used to find the required gains.

$$K_p = 0.6K_u$$
$$K_i = {2K_p}/{\omega_n}$$
$$K_d = {K_p\omega_n}/{8} \tag{7}$$

7.2 Manual tuning

Several design criteria must be considered when utilizing the manual tuning technique. Rise time (t_r), damping ratio (ζ), and settling time (t_s) are the design characteristics required and may be used in the equation in (8) to find the new gains.

$$T = {10}/{\zeta\omega_n}$$
$$K_p = J\left(\omega_n^2 + {2\zeta\omega_n}/{T}\right)$$
$$K_i = J\left({\omega_n^2}/{T}\right)$$
$$K_d = J\left(2\zeta\omega_n + {1}/{T}\right) \tag{8}$$

7.3 Tuning using the linear quadratic regulator function

The LQR function in MATLAB requires the state space form of the control system. Using the form $\dot{x} = Ax + Bu$ and $y = Cx + Du$ the state space form of the torque equation in the inertial frame can be constructed. The state space from in Eq. (9) was developed and used to derive the gains from the LQR function.

$$A = \begin{bmatrix} 0 & 1 \\ 0 & 0 \end{bmatrix}$$
$$B = \begin{bmatrix} 0 \\ J^{-1} \end{bmatrix}$$
$$C = \begin{bmatrix} 1 & 0 \end{bmatrix}$$
$$D = \begin{bmatrix} 0 \end{bmatrix} \tag{9}$$

The three tuning techniques were completed, and the gain values were calculated. These gains have been compiled and entered in **Table 2** [5].

Using the gains found in **Table 2**, three differing step functions can be found and analyzed. Ziegler-Nichols was found to be the optimal tuning method for the controllers. The LQR function is the worst way of tuning the controller. The overshoot is largest of the three tuning methods and the settling time takes longer than 100 s [5].

Case	Tuning technique	K_p	K_i	K_d
1	Ziegler-Nichols	16.20	0.78	84.65
2	Manual	36.76	1.41	55.67
3	LQR function	1.00	0.10	11.45

Table 2.
Gain solutions for different tuning techniques.

8. Plotting singularity regions with mixed skew angles

A series of mixed skew profiles were selected to perform initial analysis on. Upon investigation, certain profiles were further analyzed to see how they would be advantageous for a spacecraft with a specific maneuver requirement such as maneuver in pitch, roll, or yaw. **Figure 2** demonstrates how these skew angles (β) can change for each of the CMGs in the 3/4 configuration. When these skew angles are altered, new singularity regions are developed and create a hazard for spacecraft control. Five series of singularity plots have been generated to attain an initial picture of how the skew angles affect those singularity regions (**Tables 3–7**).

Profile	CMG 1-β	CMG 2-β	CMG 3-β
1	15	30	60
2	30	15	60
3	30	60	15
4	15	60	30
5	60	15	30
6	60	30	15

Series 1. Using skew angles (β)-15, 30, 60°.

Table 3.
Series 1 CMG β angle configurations.

Profile	CMG 1-β	CMG 2-β	CMG 3-β
1	20	40	80
2	20	80	40
3	40	20	80
4	40	80	20
5	80	20	40
6	80	40	20

Series 2. Using skew angles (β)-20, 40, 80°.

Table 4.
Series 2 CMG β angle configurations.

Profile	CMG 1-β	CMG 2-β	CMG 3-β
1	30	60	90
2	30	90	60
3	60	30	90
4	60	90	30
5	90	30	60
6	90	60	30

Series 3. Using skew angles (β)-30, 60, 90°.

Table 5.
Series 3 CMG β angle configurations.

Profile	CMG 1-β	CMG 2-β	CMG 3-β
1	0	45	90
2	0	90	45
3	45	0	90
4	45	90	0
5	90	0	45
6	90	45	0

Series 4. Using skew angles (β)-0, 45, 90°.

Table 6.
Series 4 CMG β angle configurations.

Profile	CMG 1-β	CMG 2-β	CMG 3-β
1	0	30	60
2	0	60	30
3	30	0	60
4	30	60	0
5	60	3	30
6	60	30	0

Series 5. Using skew angles (β)-0, 30, 60°.

Table 7.
Series 5 CMG β angle configurations.

The singularity plots associated with these series are found in Appendix A of this report. Each of these plots was analyzed to see breadth and depth of singularity surfaces internal to the saturation region of the 3/4 CMG configuration depicted in **Figure 2**.

9. Determining singularity free regions

The five series of singularity plots were observed to determine internal singularity free regions. The objective was to find an internal region in which the spacecraft could maneuver without running into a singularity. Also, if there was a singularity, would the spacecraft be capable of passing through a small amount of singularities in
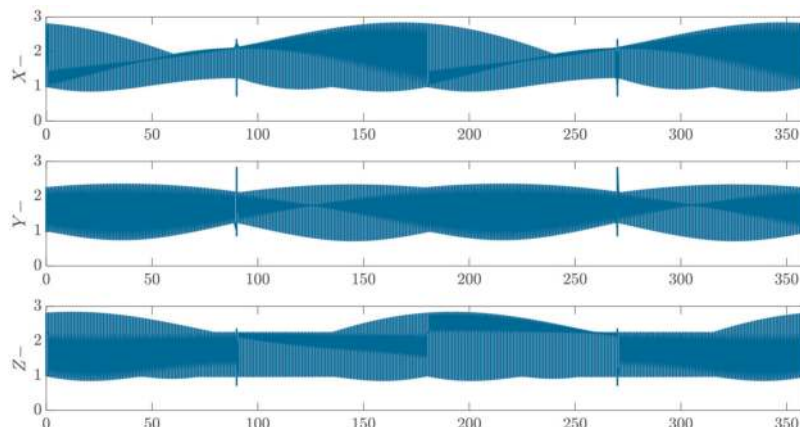
Figure 5.
Singularity regions in the X-, Y- and, Z rotation for 0, 45, and 90° skew angles.

order to continue maneuvering to a commanded rotation. Singularity penetration is a feasible concept however the goal of this paper was to use it sparingly.

The singularity regions found in **Figure 5** demonstrate how with varied skew angles new singularity free regions may be discovered and utilized to a spacecraft designer's advantage. Although the angular momentum plotted in **Figure 5** first interacts with a singularity at a value of 0.73, it only hits the singularity for an instance. Using singularity penetration logic discussed in part VI may allow the spacecraft to operate in an angularity momentum regime at $H = 1.0$ or greater.

The maximum angular momentum achieved by the mixed skew configurations in series 1–5 has been plotted and the data was consolidated into **Table 8**.

Series	CMG 1-β	CMG 2-β	CMG 3-β	Max H*
1	15	30	60	0.54
	30	15	60	0.51
	30	60	15	0.16
	15	60	30	0.16
	60	15	30	0.51
	60	30	15	0.54
2	20	40	80	0.34
	20	80	40	0.17
	40	20	80	0.33
	40	80	20	0.17
	80	20	40	0.33
	80	40	20	0.53
3	30	60	90	0.12
	30	90	60	0.41
	60	30	90	0.51
	60	90	30	0.41
	90	30	60	0.51
	90	60	30	0.25
4	0	45	90	0.73
	0	90	45	0.22
	45	0	90	0.41
	45	90	0	0.22
	90	0	45	0.41
	90	45	0	0.73
5	0	30	60	0.52
	0	60	30	0.39
	30	0	60	0.52
	30	60	0	0.39
	60	0	30	0.52
	60	30	0	0.53

*Maximum Ang. Momentum (H) in singularity free region.

Table 8.
Series 5 CMG β angle configurations.

10. Conclusion

Mixed skew angles bring a new variety and flexibility in spacecraft design. These new CMG configurations enable engineers to now explore new singularity free regions and push spacecraft to possibly operate with higher levels of momentum.

As seen in **Table 8**, when the opposing CMG configurations have a dramatic change in configuration, the Angular Momentum is typically higher. This is not always the case, as seen in series 3, configurations 1 and 6 (the most dramatic change between CMG 1 and 3 in the series) demonstrate the worst angular momentum possibility. Several of these configurations cater to different requirements of the spacecraft. For example, Series 3 Configuration 5 (ref. Appendix A) may be more suitable for a spacecraft that requires movement about the roll and yaw axes. Series 3 Configuration 2 may be more suitable for pitch and roll spacecraft. Appendix A is meant to be used by spacecraft designers to design a spacecraft suitable to the requirements needed.

Appendix A

Singularity Plots
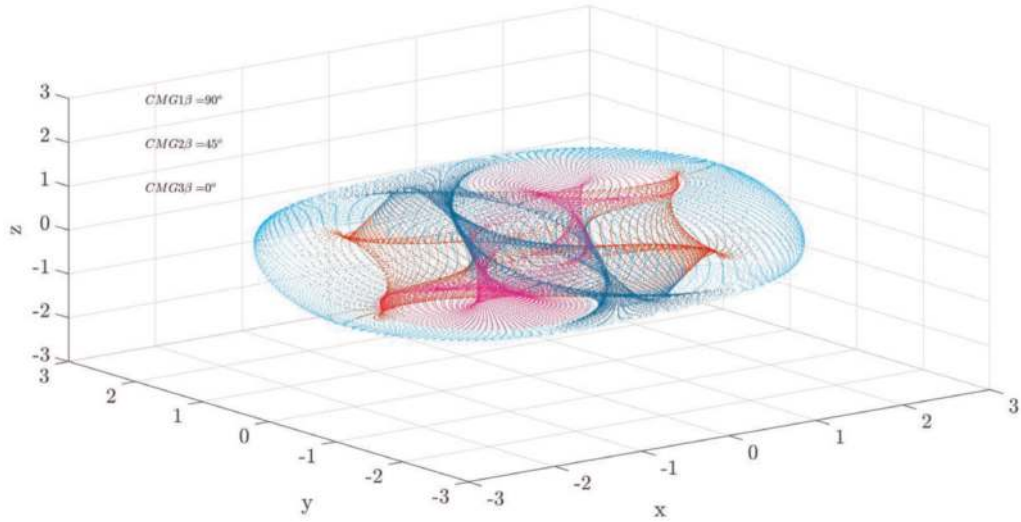Series 1:
Configuration 1:
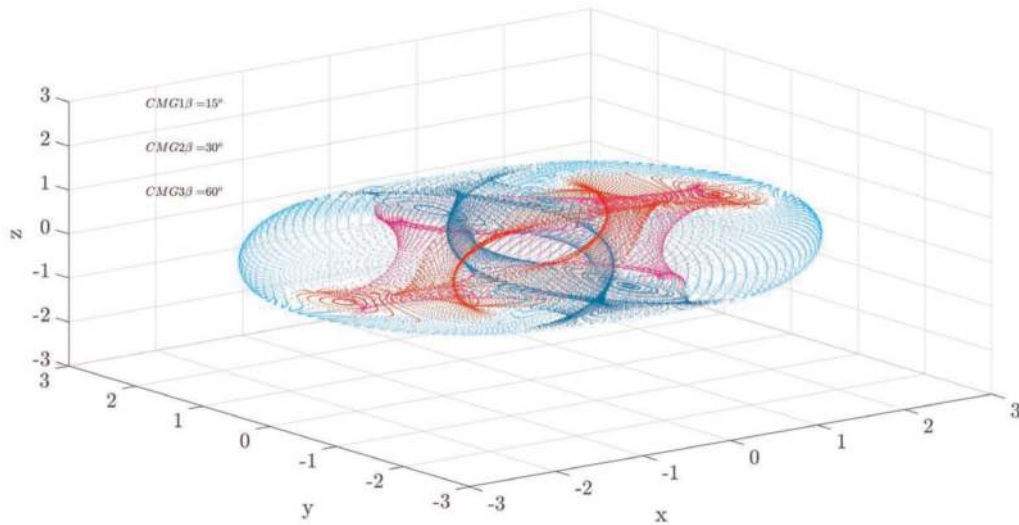
Configuration 2:

Configuration 3:

$CMG1\beta = 30°$
$CMG2\beta = 60°$
$CMG3\beta = 15°$

Configuration 4:

$CMG1\beta = 15°$
$CMG2\beta = 60°$
$CMG3\beta = 30°$

Configuration 5:

$CMG1\beta = 60°$
$CMG2\beta = 15°$
$CMG3\beta = 30°$

Configuration 6:

$CMG1\beta = 60°$
$CMG2\beta = 30°$
$CMG3\beta = 15°$
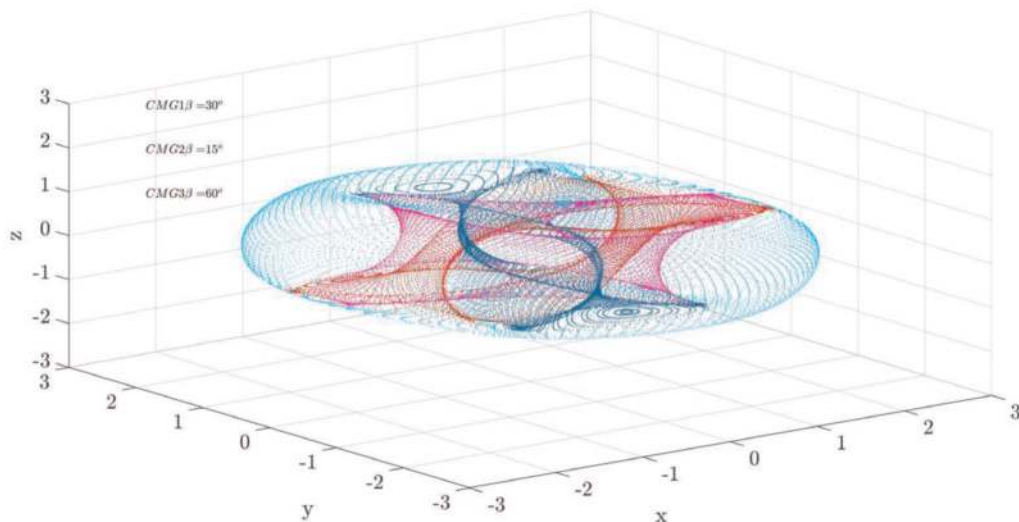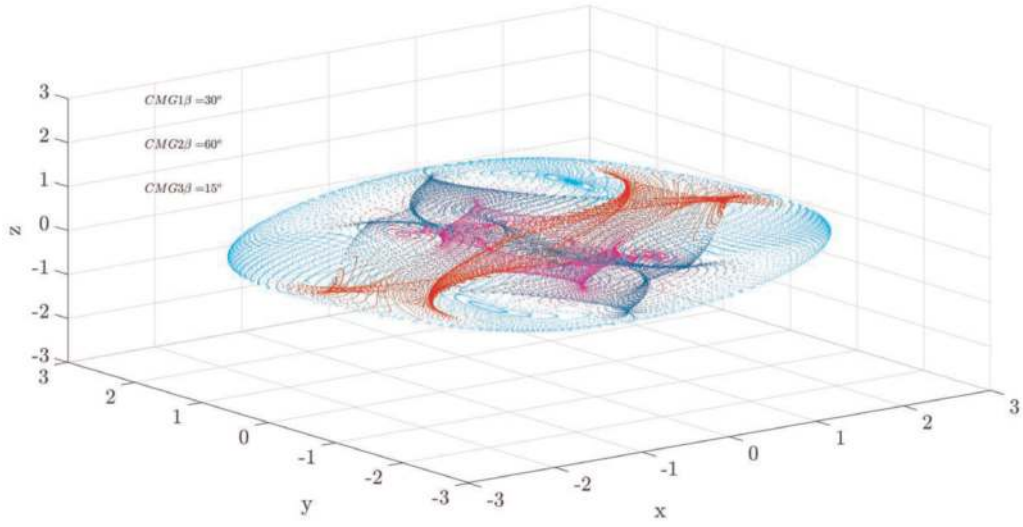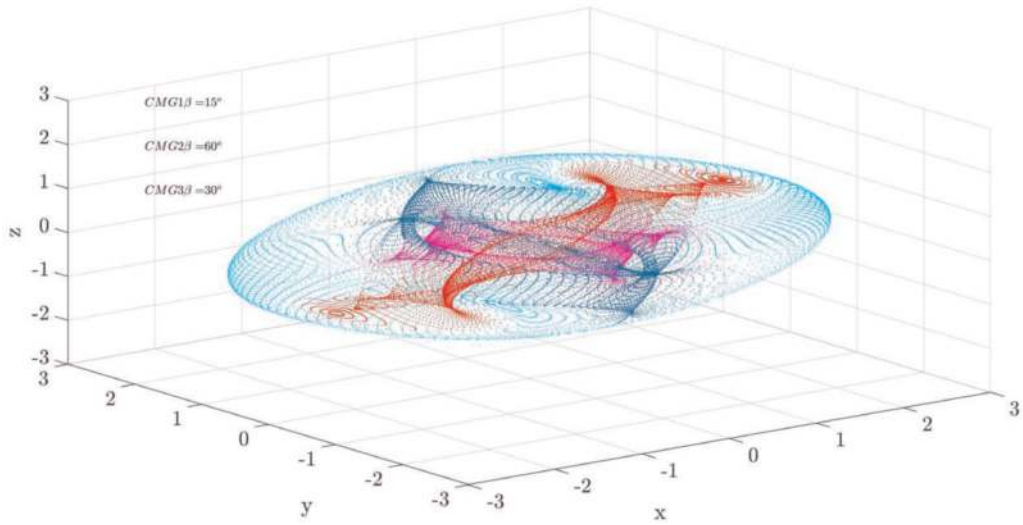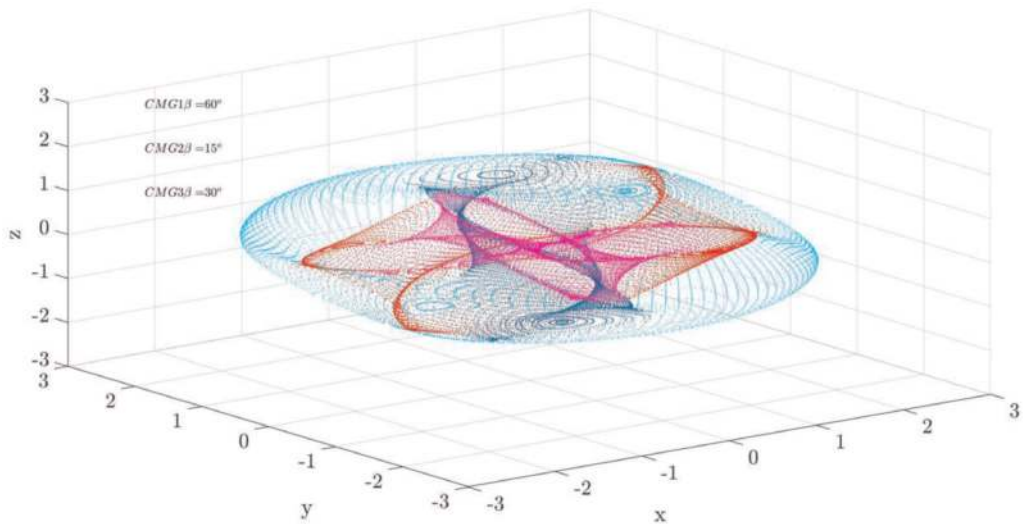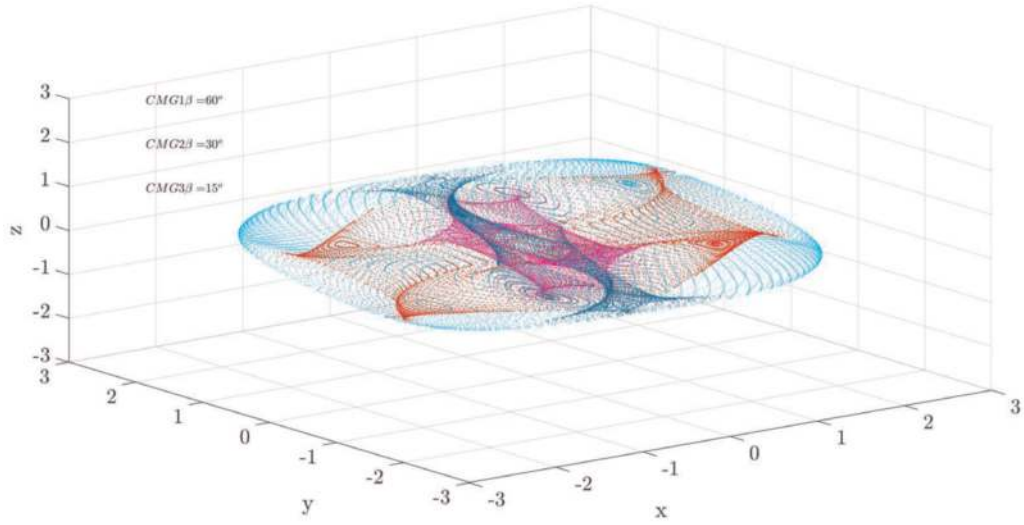
Series 2:
Configuration 1:
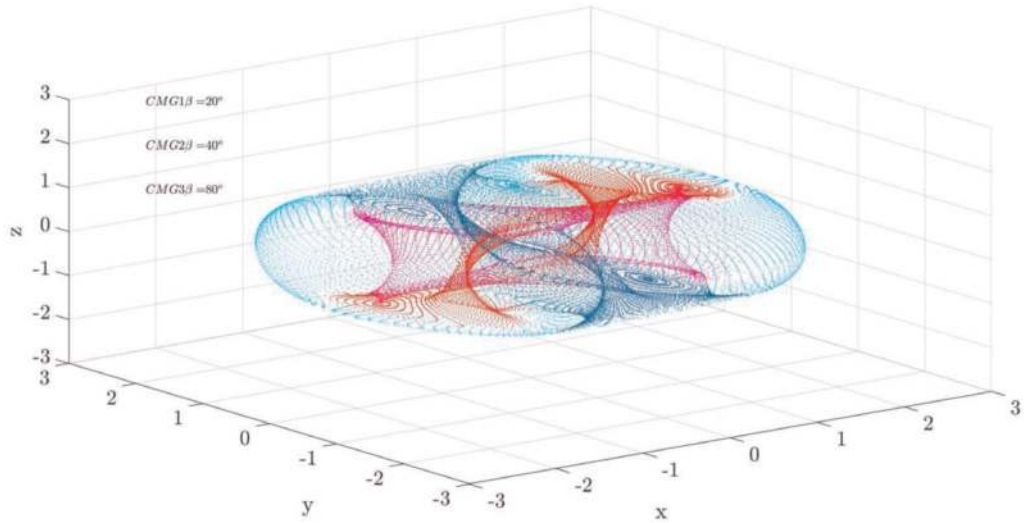
$CMG1\beta = 20°$
$CMG2\beta = 40°$
$CMG3\beta = 80°$

Configuration 2:

$CMG1\beta = 20°$
$CMG2\beta = 80°$
$CMG3\beta = 40°$
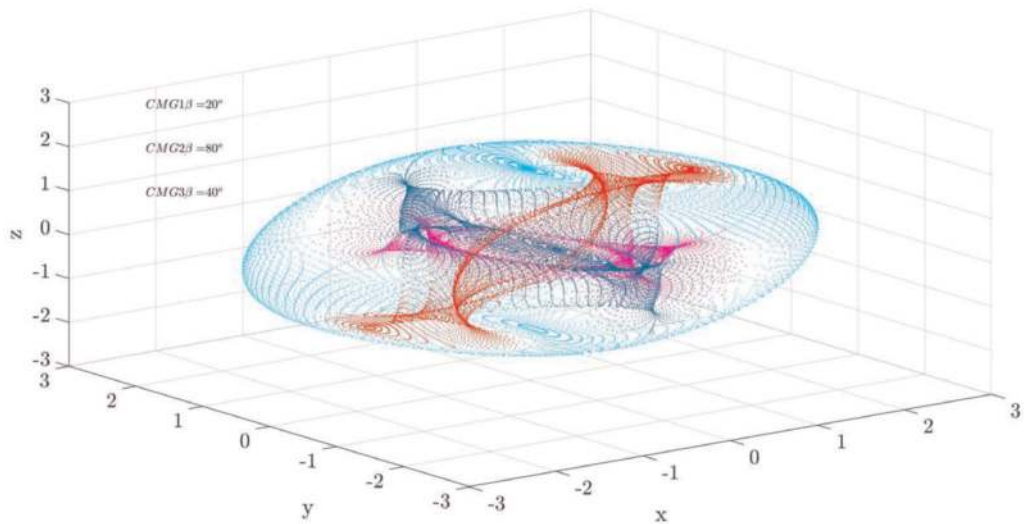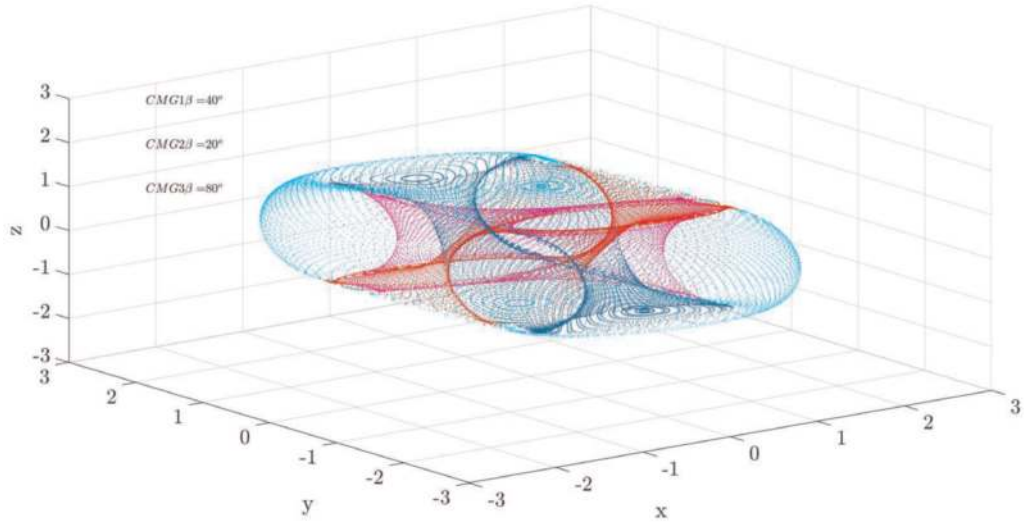
Configuration 3:
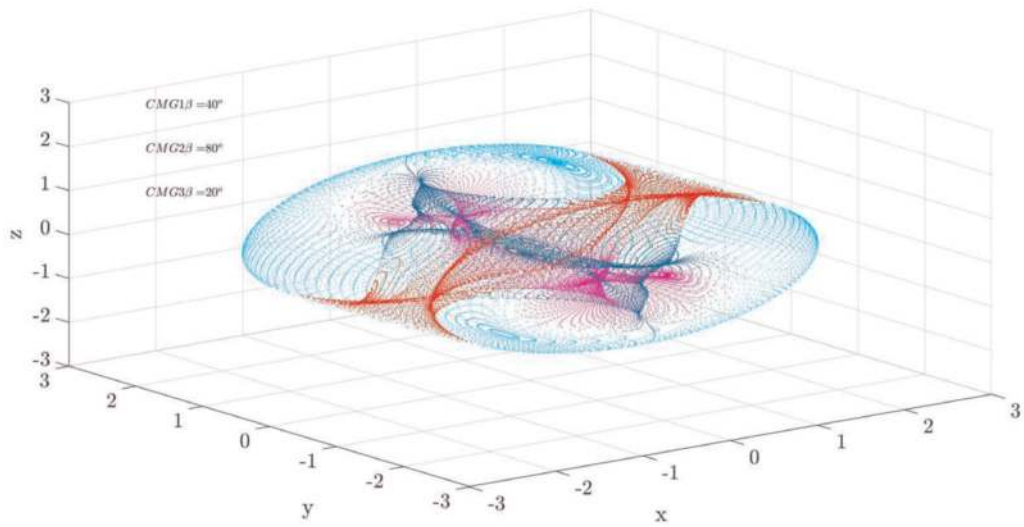
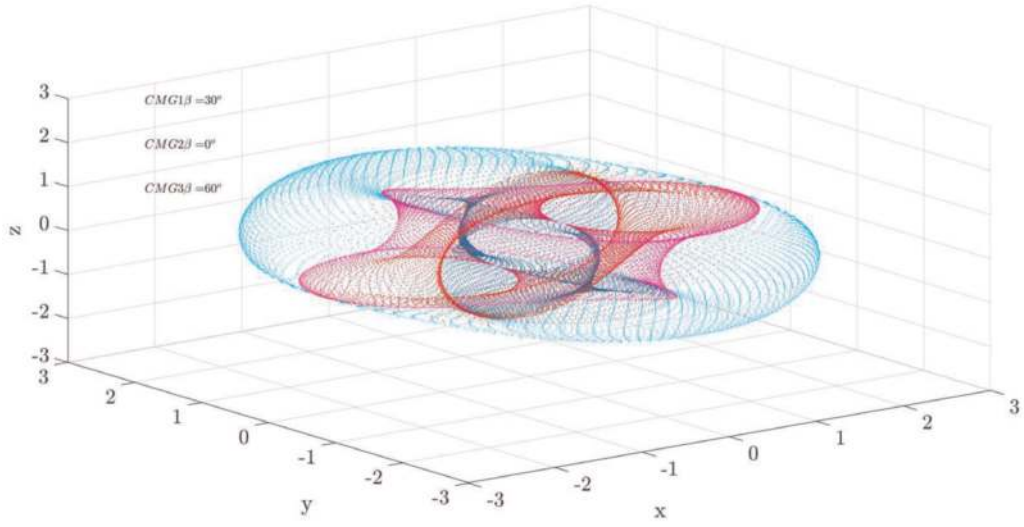Configuration 4:
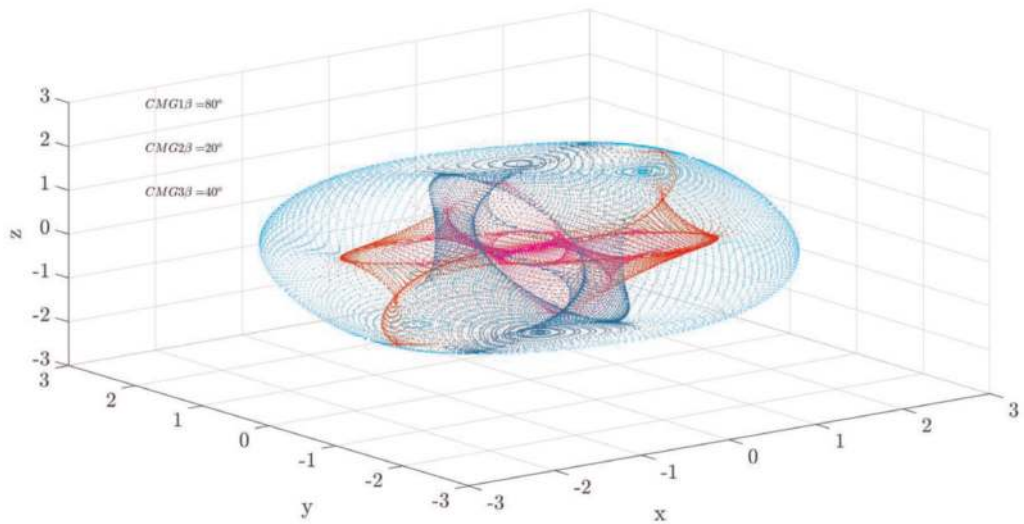
Configuration 5:
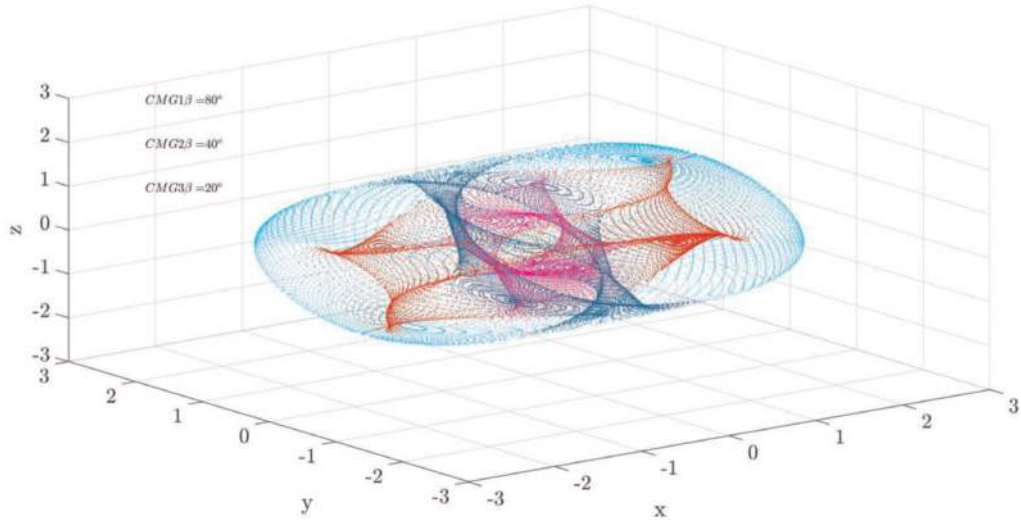
Configuration 6:

Series 3:
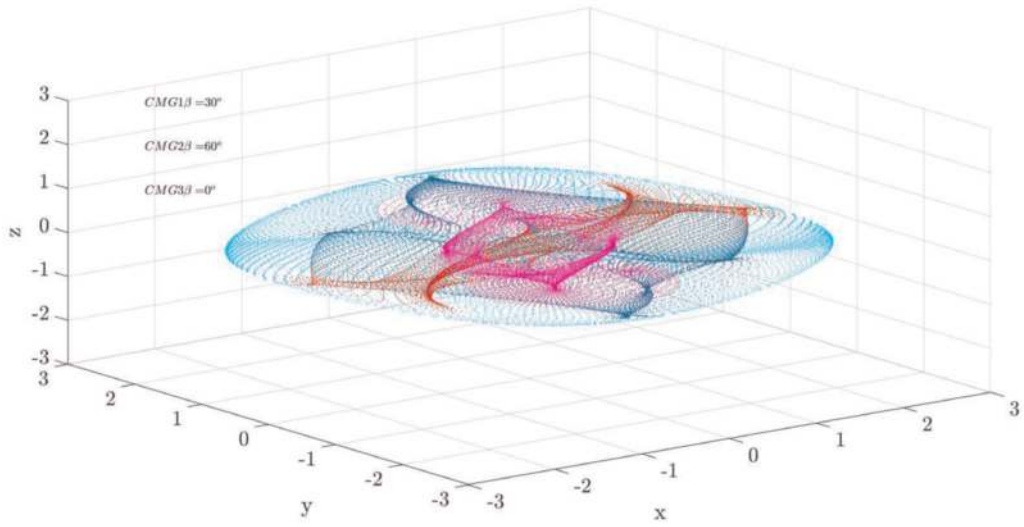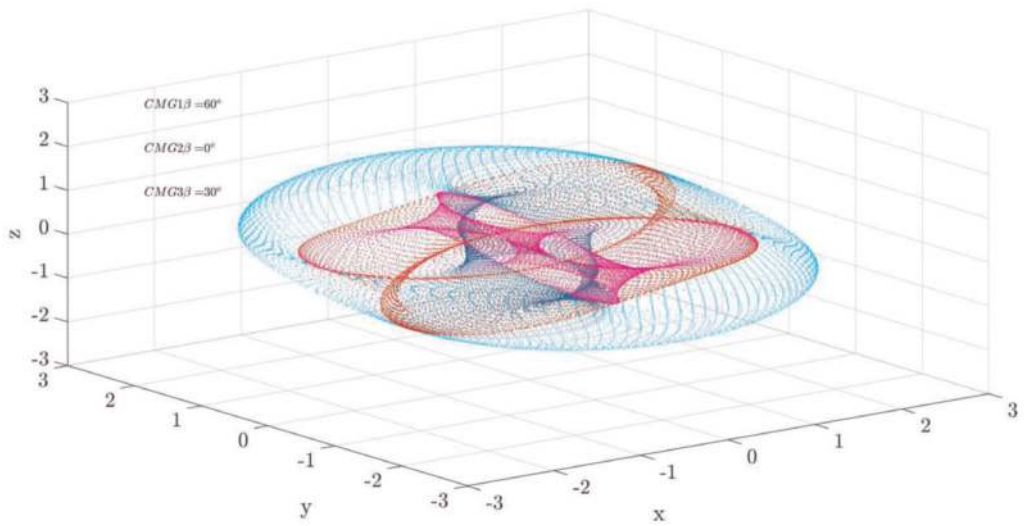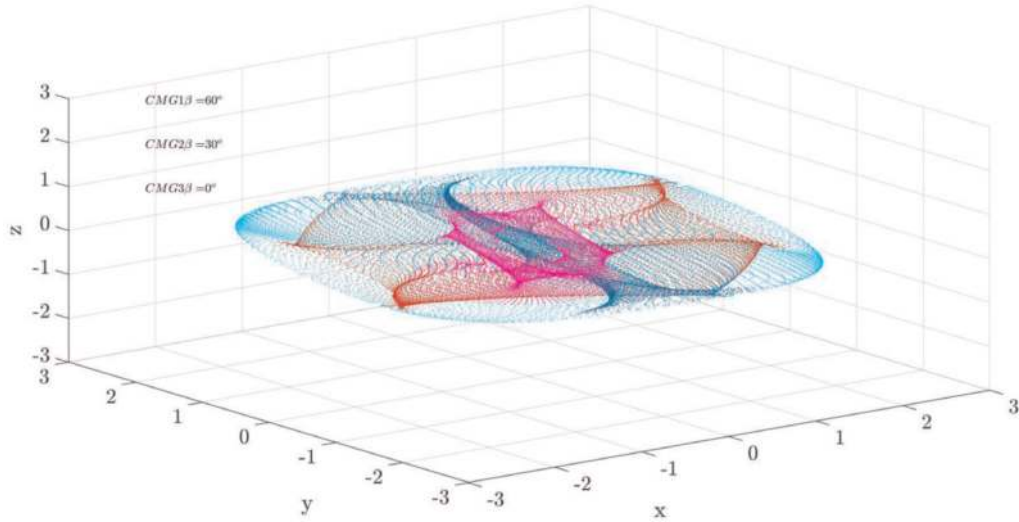Configuration 1:
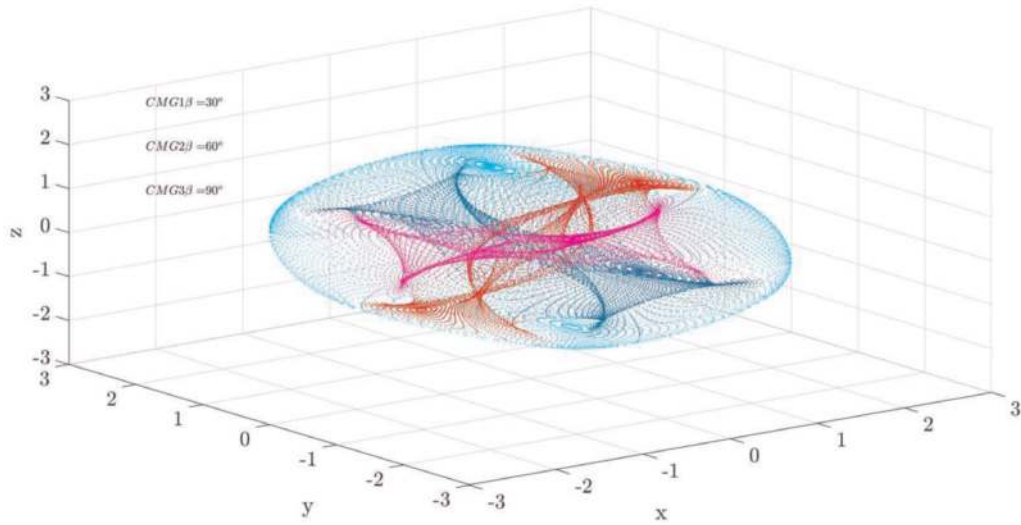
Configuration 2:
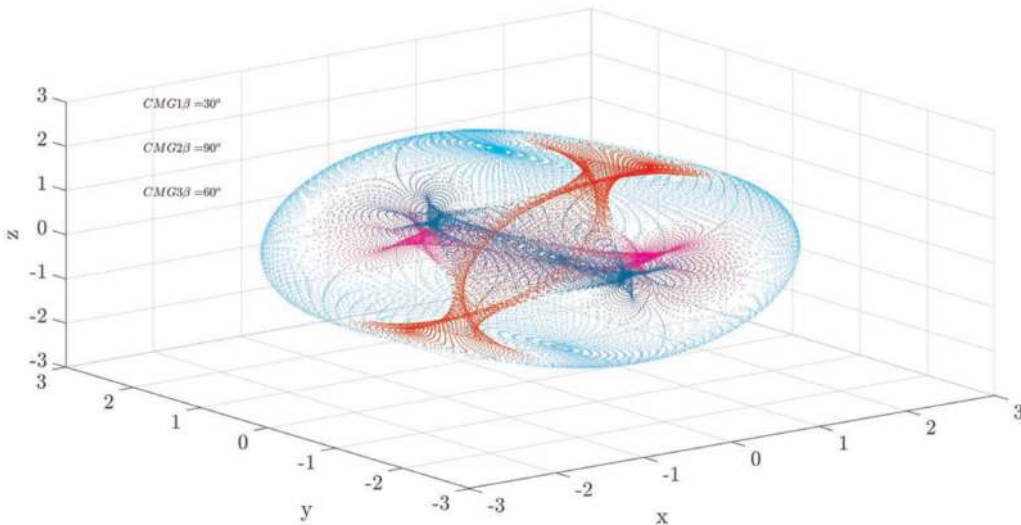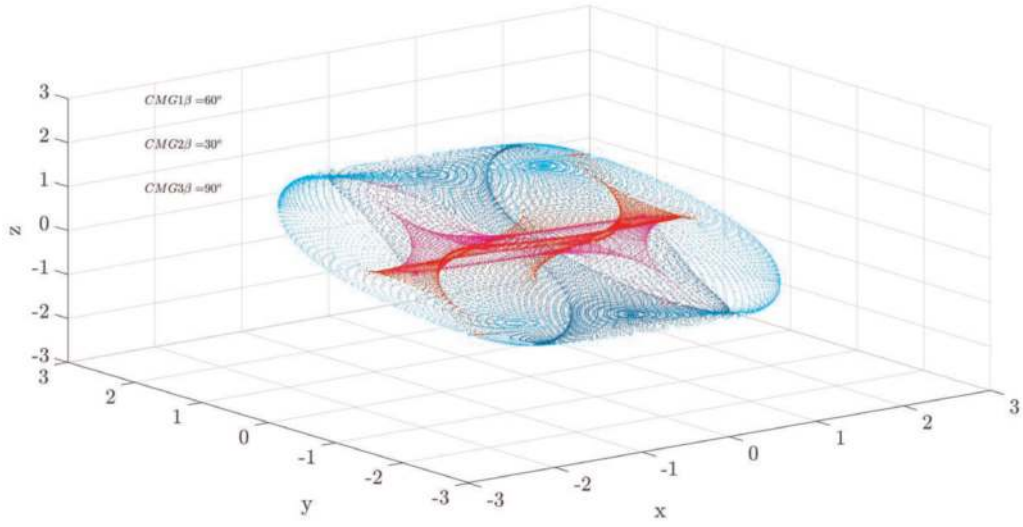
Configuration 3:
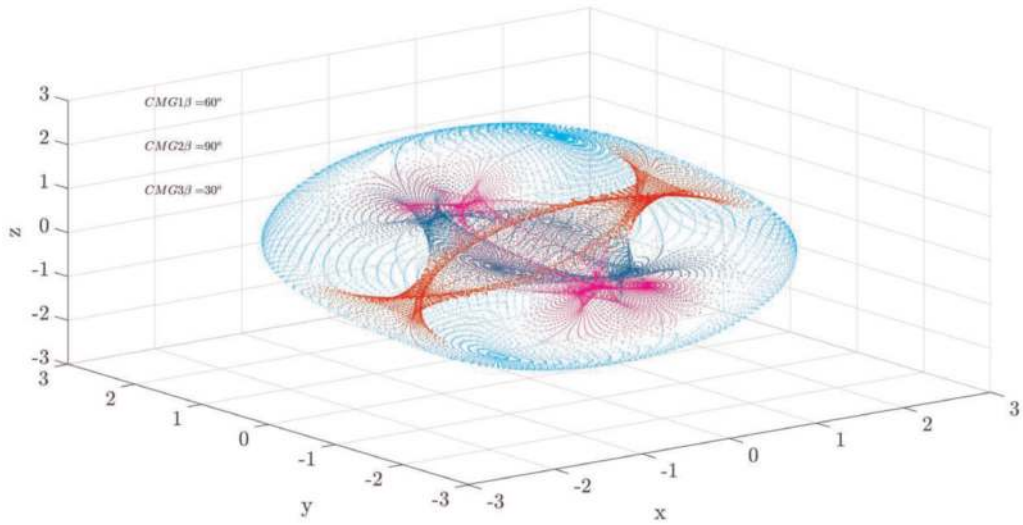
Configuration 4:
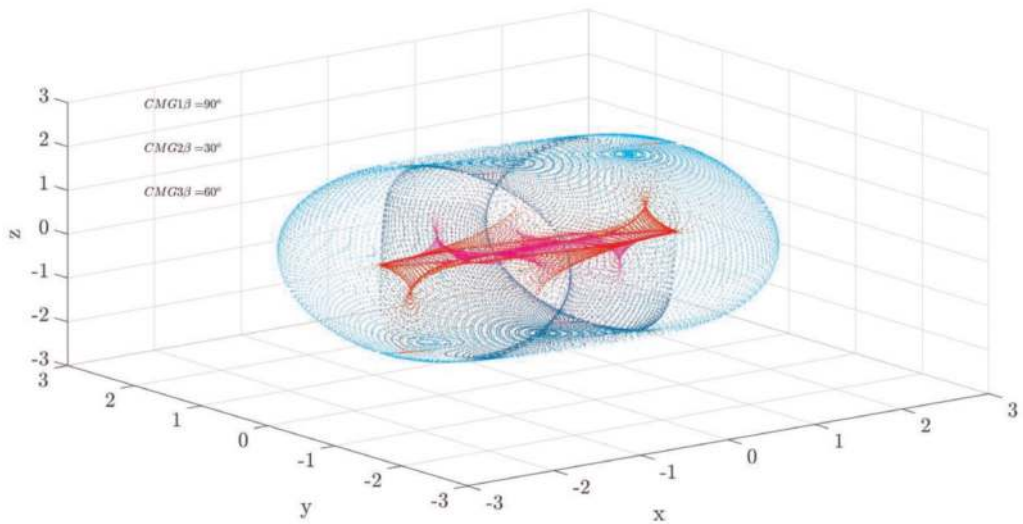
Configuration 5:
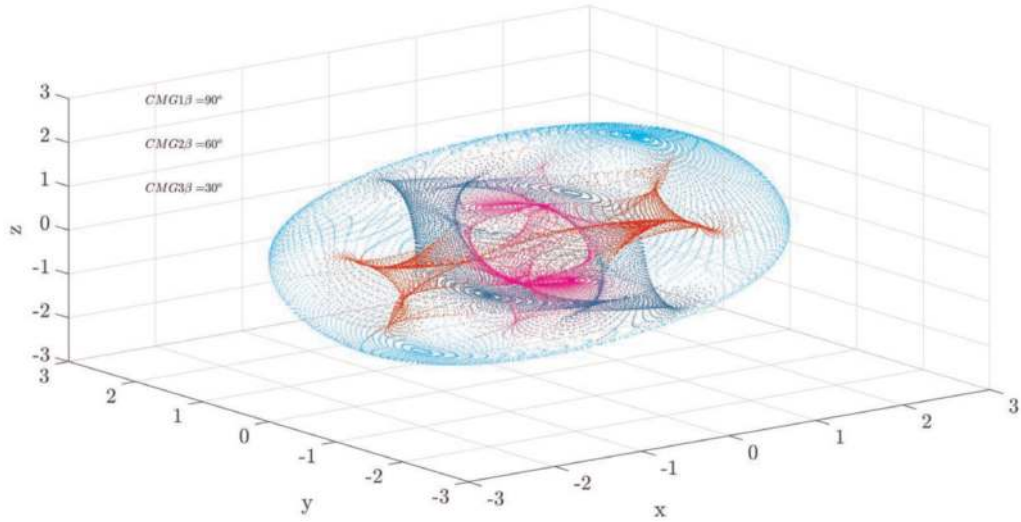
Configuration 6:

Series 4:
Configuration 1:
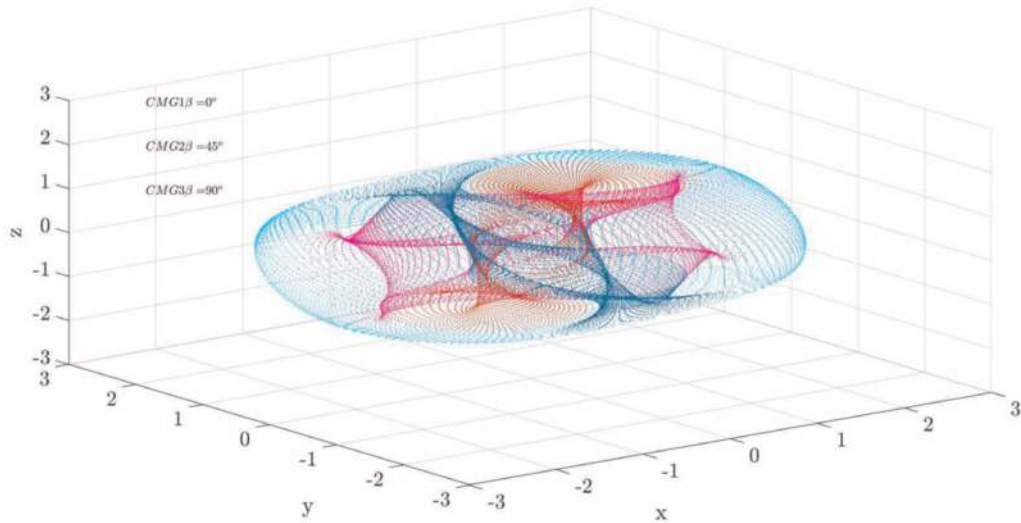
Configuration 2:
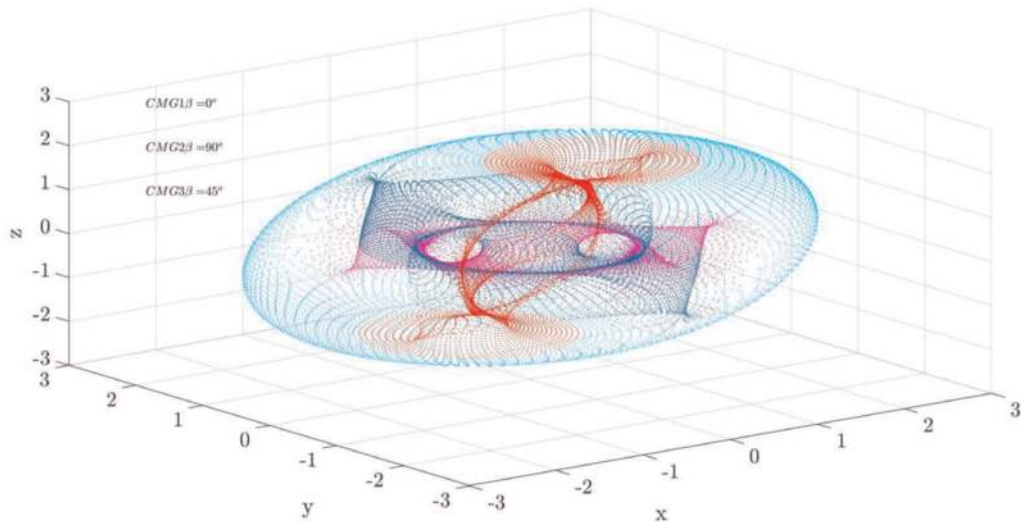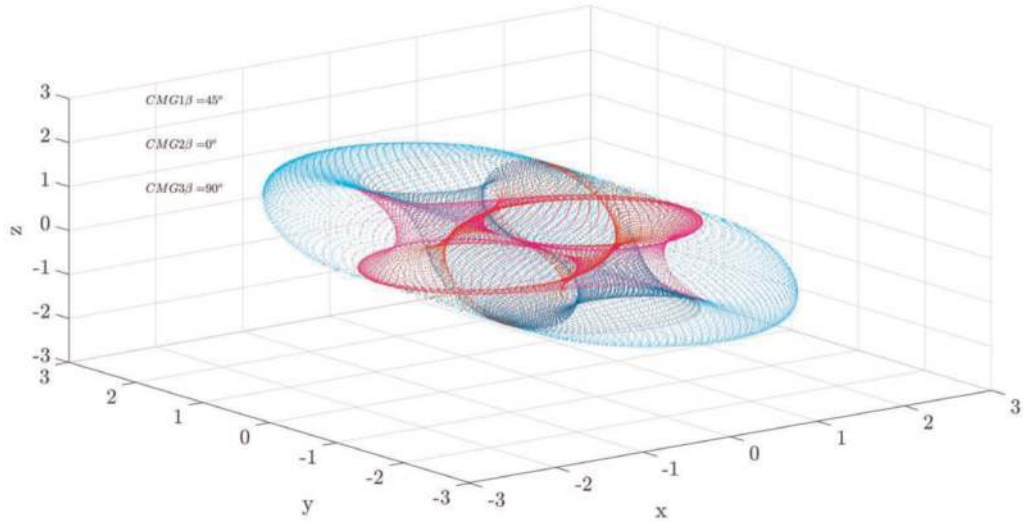
Configuration 3:
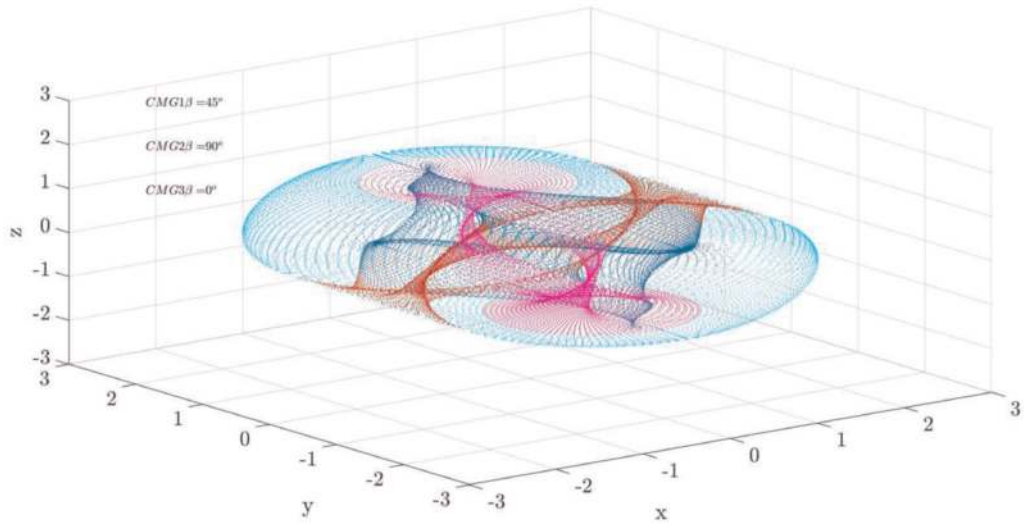
Configuration 4:
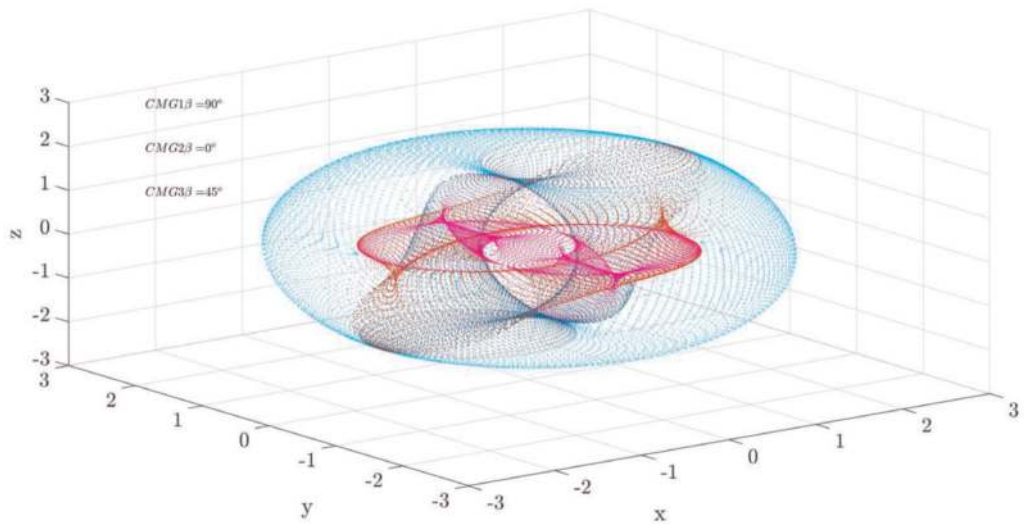
Configuration 5:

Configuration 6:

Series 5:
Configuration 1:
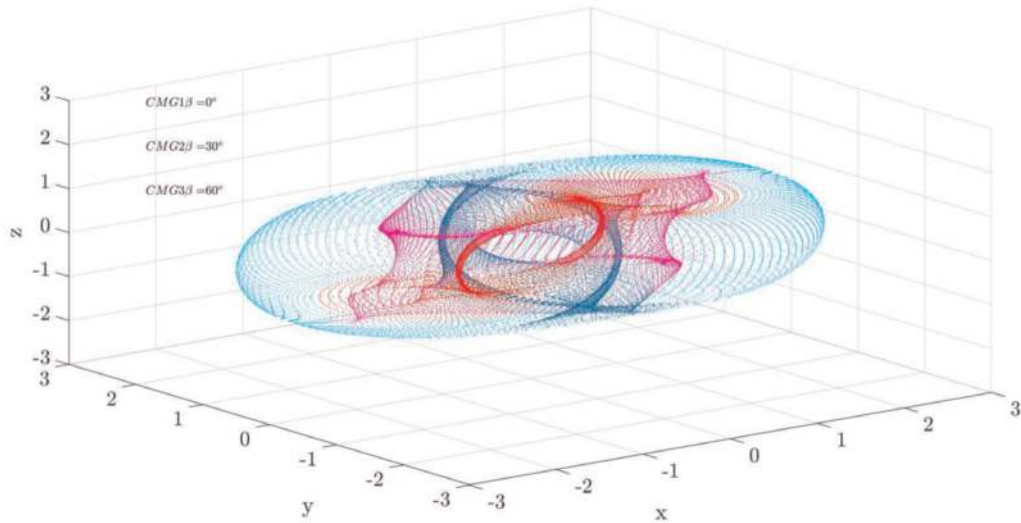
Configuration 2:
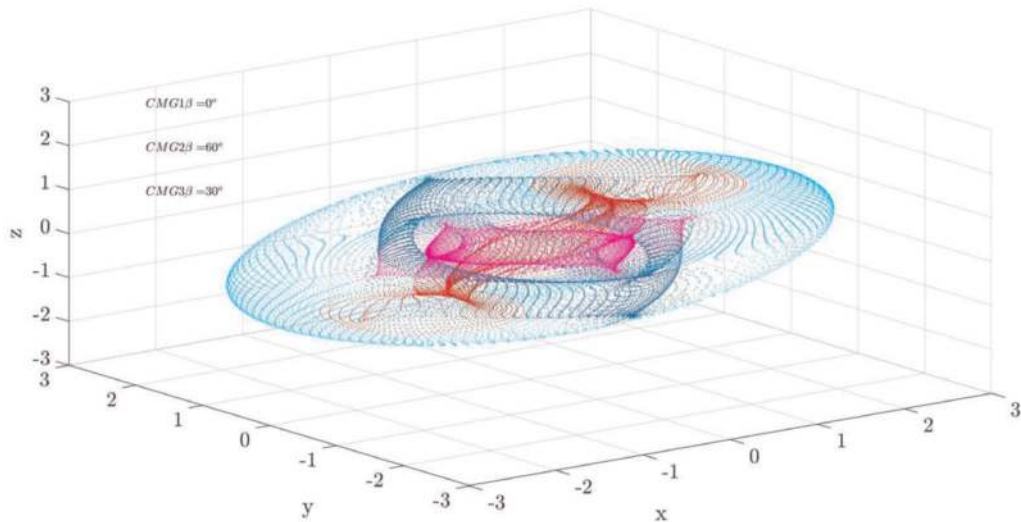
Configuration 3:

Configuration 4:

Configuration 5:

Configuration 6:

Author details

Jonathan W. Lang
Naval Post Graduate School, United States

*Address all correspondence to: jwlang@nps.edu

IntechOpen

References

[1] Lang J. CMG singularities in a 3/4 configuration. AE3818 Spacecraft Attitude, Determination, and Control Report #1; 2019

[2] Lang J. Singularities in a 3/4 configuration. AE3818 Spacecraft Attitude, Determination, and Control Report #2; 2019

[3] Lang J. Increased CMG capability using singular penetration logic. AE3818 Spacecraft Attitude, Determination, and Control Report #3; 2019

[4] Lang J. Spacecraft kinematics in a 3-2-1 rotation. AE3815 Spacecraft Rotational Mechanics Report #2; 2019

[5] Lang J. Tuning for PID and PDI controllers. AE3818 Spacecraft Attitude, Determination, and Control Report #4; 2019